Nuclear Materials and Energy 20 (2019) 100704

Contents lists available at ScienceDirect

Nuclear Materials and Energy

journal homepage: www.elsevier.com/locate/nme

Deuterium retention in silicon carbide, SiC ceramic matrix composites, and SiC coated graphite

Markus T. Koller[a], James W. Davis[*,b], Megan E. Goodland[b], Tyler Abrams[c], Sean Gonderman[c], Georg Herdrich[a], Martin Frieß[d], Christian Zuber[d]

[a] Institute of Space Systems (IRS), Pfaffenwaldring 29, Stuttgart 70569, Germany
[b] University of Toronto Institute for Aerospace Studies (UTIAS), 4925 Dufferin Street, Toronto, Ontario, M3H 5T6, Canada
[c] General Atomics, 3550 General Atomics Court, San Diego, CA 92121-1122, USA
[d] Institute of Structures and Design, German Aerospace Center (DLR), Pfaffenwaldring 38-40, Stuttgart 70569, Germany

ARTICLE INFO

Keywords:
Deuterium Retention
Silicon Carbide
Ceramic Composite Materials
Low Z Materials

ABSTRACT

Silicon Carbide (SiC) is a low Z material discussed as an alternative to graphite for fusion devices. The retention of hydrogenous species is an important plasma-surface interaction property. Deuterium was implanted into SiC, SiC_f/SiC, C_f/C-SiC and SiC coated graphite under various particle energy and substrate temperature conditions. A TDS process was used to characterise the deuterium retention of the implanted specimens. While all SiC materials show elevated retention levels compared to graphite, the differences are limited to about a factor of two over the range of parameters investigated.

1. Introduction

Silicon Carbide (SiC) is a ceramic material with various favourable properties for aerospace and fusion applications. The high melting point as well as the chemical stability suggest the use of SiC in high temperature, corrosive environments. As a “low-Z” material, SiC can be tolerated at higher concentrations as an impurity in fusion plasmas and further has favourable neutron irradiation properties. Moreover, SiC exhibits good electrical and thermal conductivity in comparison with other ceramic materials [1]. A disadvantage of SiC as well as most ceramics is the low mechanical shock tolerance and the poor manufacturability of large three dimensional structures. A possible solution to these issues could be the use of Ceramic Matrix Composite (CMC) materials. These materials gained popularity in the recent decades and have already been considered as a structural material for the ARIES-AT power plant concept [2]. Besides the erosion yield and the codeposition properties, the hydrogen retention properties are among the most important plasma-surface interaction effects. The erosion yield, especially of bulk SiC, but also of SiC_f/SiC and SiC coated materials has been extensively studied since the 1970s by multiple authors. However, only little research on hydrogen retention has been conducted on SiC [3–5], SiC coated [6] and SiC_f/SiC CMC materials [7]. The related topic of hydrogen transport in SiC based materials has also been the subject of previous investigation [e.g. 8, 9]. The objective of this research has thus been the characterisation and comparison of the deuterium retention properties of the aforementioned materials.

2. Materials and methods

2.1. Materials

Several promising silicon carbide based materials were investigated ranging from monolithic C-based ceramics such as sintered SiC from Ortech Ceramics and CVD-SiC coated graphite manufactured by General Atomics, both with low damage tolerance, as well as fibre reinforced ceramic matrix composite materials like carbon fibre reinforced silicon carbide (C_f/C-SiC) and SiC fibre reinforced SiC matrix composites (SiC_f/SiC or SiC/SiCN). According to Mainzer et al. [10], the SiC/SiCN CMC composite was produced via Polymer Infiltration and Pyrolysis process (PIP) using SA3 fibres from Tyranno Corp. (Jp) as well as the Si-based polymer PSZ10 from Clariant SE, Germany. The C_f/C-SiC was manufactured by infiltration of a porous C_f/C composite with liquid silicon as described by Frieß et al. [11]. The density is smaller than the SiC_f/SiC, even though the material contains only small amounts of porosities, because of the higher content of the light carbon fibres. Further, a reference sample made of HPG99 pyrolytic graphite from Union Carbide was tested. The aforementioned materials are listed in Table 1.

* Corresponding author.
E-mail addresses: mkoller@irs.uni-stuttgart.de (M.T. Koller), jwdavis@starfire.utias.utoronto.ca (J.W. Davis).

https://doi.org/10.1016/j.nme.2019.100704
Received 8 July 2019; Received in revised form 21 August 2019; Accepted 21 August 2019
Available online 13 September 2019

Table 1
Origin and properties of the tested materials.

Material type	Manufacturing process	Manufacturer	Density [g/cm^3]	Porosity [%]
SiC	Sintering	Ortech Ceramics	3.15	~ 0
SiC_f/SiC[a]	Polymer infiltration and pyrolysis	DLR Stuttgart	2.18	< 8 (7.21)
C_f/C-SiC	Liquid silicon infiltration	DLR Stuttgart	1.87	< 2 (1.39)
SiC coated C	Chemical vapour deposition	General Atomics	3.21[b]	-
C	Pyrolysis	Union Carbide	2.2	-

[a] Alternative name SiC/SiCN due to nitrogen remnants from polysilazane precursor.
[b] 125 ± 25 μm SiC deposition layer, density of graphite substrate ~ 1.76 g/cm^3.

All samples except the SiC coated graphite were cut into specimens of a size of 5 × 7 × 0.5 mm^3 and were mechanically polished to obtain a mirror finish on both sides of the specimens. The thickness after polishing was approximately 0.4 mm to 0.5 mm which was determined to be the smallest practical thickness in order to avoid cracking during the handling of the bulk SiC specimens. The SiC coated specimen were tested in the "as received" condition. Moreover, all specimens were annealed at 1500 K for 30 min in a separate vacuum system prior to implantation in order to remove surface and near-surface contaminants.

Unfortunately, the surface composition was not assessed for any of the materials at any stage of the experiments. However, it can be assumed that the initial surface composition before annealing for SiC and SiC coated graphite is close to equilibrium, while the surface composition of the CMC materials strongly depends on the surface features in the irradiated area. The carbon fibres in the C_f/C-SiC material for example increase the C to Si ratio significantly while the SiC matrix tends to push the surface composition closer to equilibrium. Also, it is expected that the surface composition could change during heat treatment and deuterium irradiation. For example, silicon enrichment due to hydrocarbon formation during deuterium ion irradiation was observed by Oya et al. [5].

2.2. Methods

The implantations were performed with a D_3^+ ion beam at the dual ion beam facility of UTIAS as described in detail by Haasz and Davis [12]. Either the ion energy, the substrate temperature or the fluence were varied in the respective measurement series as explained in Table 2.

The irradiated specimen were transported between the vacuum vessels of the ion beam accelerator and the Thermal Desorption Spectroscopy (TDS) system through air. A Papyex (manufactured by Mersen) heating cradle was utilised to heat the specimens at a rate of 1 K/s from room temperature to approximately 1500 K. The temperature of the irradiated specimens was inferred by using a SiC reference specimen with a type W-Re thermocouple glued onto the reference SiC specimen with high-temperature resistant, vacuum compatible Graphi-Bond^{TM}669 graphite glue and positioned next to the irradiated specimen. This method assumes that the differences in emissivity, thermal capacity and conductivity between the SiC reference specimen and all other tested samples of the same as well as different materials are reasonably similar for thin specimens. The desorption of mass 2 (H_2), mass 3 (HD), mass 4 (D_2), mass 16 (CH_4) and mass 20 (CD_4, D_2O) were monitored with both a 201RC/HAL V Hiden and a model 5221 Extrel Residual Gas Analysis (RGA) Quadrupole Mass Spectrometer (QMS). The quantification of the signals could be achieved by using D_2, CD_4 and H_2 leak bottles. Signals without leak bottles were quantified using the respective ionisation sensitivities according to Hiden and the relative pumping speed of the turbomolecular pumps for the individual species as given by Pfeiffer Vaccum. The background pressure at the start of the TDS process was below $p = 1.5{\cdot}10^{-6}$ Pa.

Table 2
Irradiation conditions of the measurement series conducted at UTIAS.

Variable	Fluence[a] Φ [D/m^2]	Particle energy E [eV/D$^+$]	Substrate temp. T [K]
Fluence	$1{\cdot}10^{21}$ – $3{\cdot}10^{24}$	1000	300
Energy[b]	$5{\cdot}10^{23}$	500 – 3000	300
Temperature	$1{\cdot}10^{24}$	1000	300 – 800

[a] Variance usually < ± 10%.
[b] E= 1000 eV/D$^+$ data points irradiated with $\Phi = 1{\cdot}10^{24}$ D/m^2.

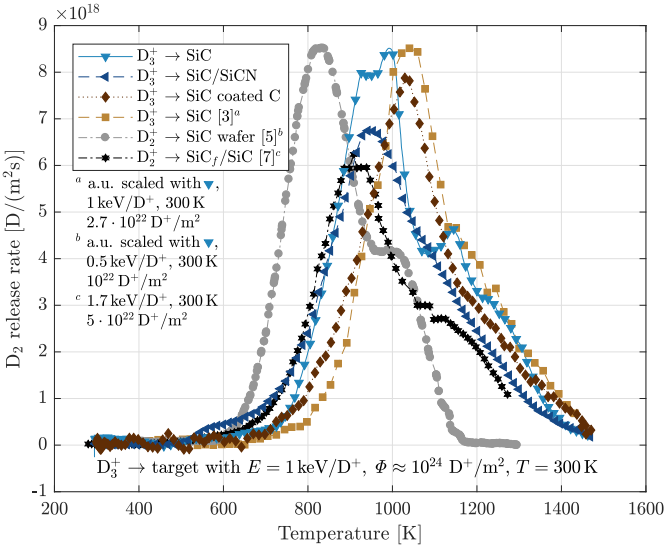

Fig. 1. Deuterium TDS profiles for SiC materials irradiated at E = 1 keV/D$^+$ and $\Phi = 10^{24}$ D/m^2.

3. Results and Discussion

A comparison of the TDS profiles of the tested bulk SiC, SiC_f/SiC and SiC coated C materials in combination with curves on SiC from Mayer et al. [3], Oya et al. [5], both scaled from a.u. to match the bulk SiC D_2 peak, as well as on SiC_f/SiC from Nobuta et al. [7] is depicted in Fig. 1. The bulk SiC curves exhibit a dominant peak which Oya et al. measured at 850 K, Mayer et al. at 1050 K and this study at approximately 930 K. Oya et al. attribute this peak to Si-D bonds as well as the secondary peak on the high temperature side to C-D bonds. The secondary peak forms a shoulder on the high temperature side of Mayer et al.'s TDS profile. The SiC TDS profiles obtained in this study exhibited a peak at the falling slope for some TDS curves and bulges or no clear pattern for others. The SiC_f/SiC results show no clear signs of a secondary peak caused by the decomposition of C-D bonds. Nobuta et al.[7] were able to see a more distinct secondary peak while otherwise both SiC_f/SiC curves match in magnitude and overall shape. Whilst the primary D_2 release peak of the SiC coated specimen matches the SiC and SiC_f/SiC data, the shoulder on the high temperature side of the profile might again indicate the presence of the secondary C-D bond peak

TDS profiles of the different tested materials irradiated at T = 300 K and E = 1 keV are depicted in Fig. 2 a)–e). The contribution of D_2, HD, CD_4 and D_2O is shown separately. While bulk SiC, SiC_f/SiC and SiC coated graphite show no significant amounts of CD_4 and D_2O desorption, C_f/C-SiC and graphite have a peak in both CD_4 and D_2O desorption at around 850 K. However, the desorption of D_2O seems to be more dominant in C_f/C-SiC than in graphite. This could be an effect of an elevated background in water vapour or a greater amounts of water

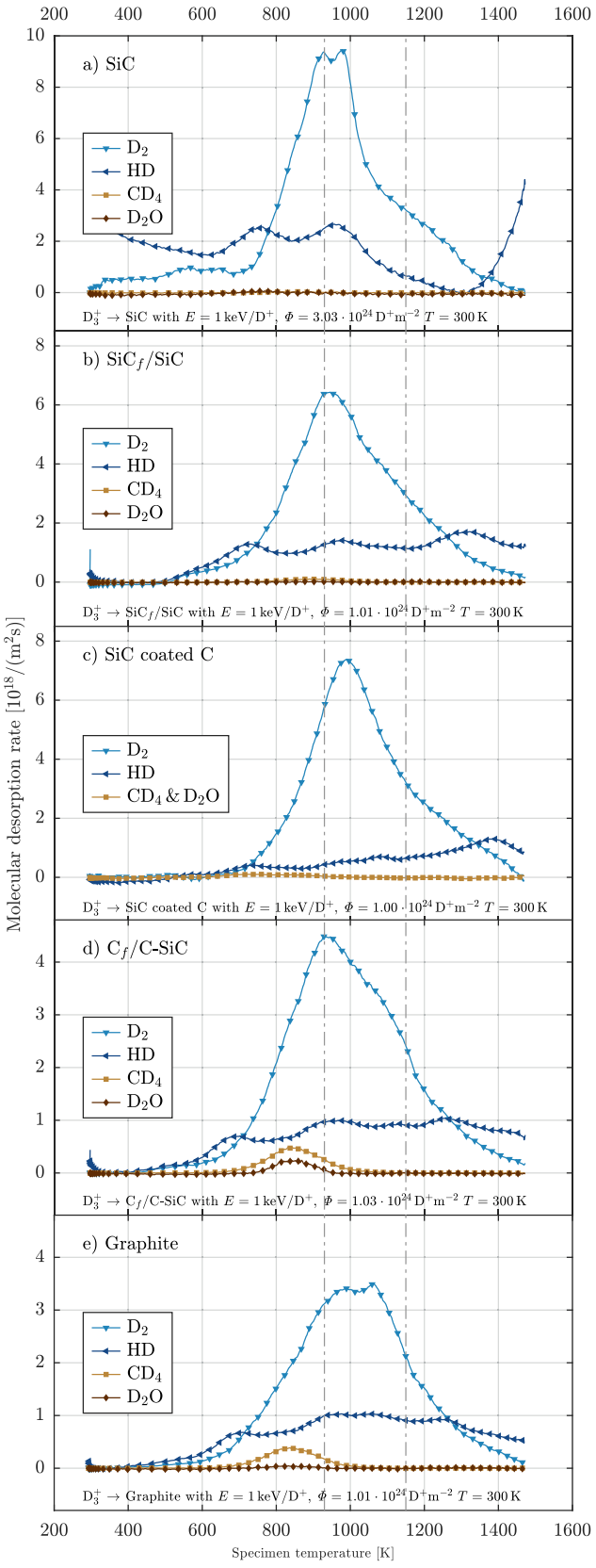

Fig. 2. D_2, HD, CD_4 and D_2O TDS profiles for all tested materials irradiated at $E = 1$ keV/D$^+$ and $\Phi \approx 10^{24}$ D/m^2.

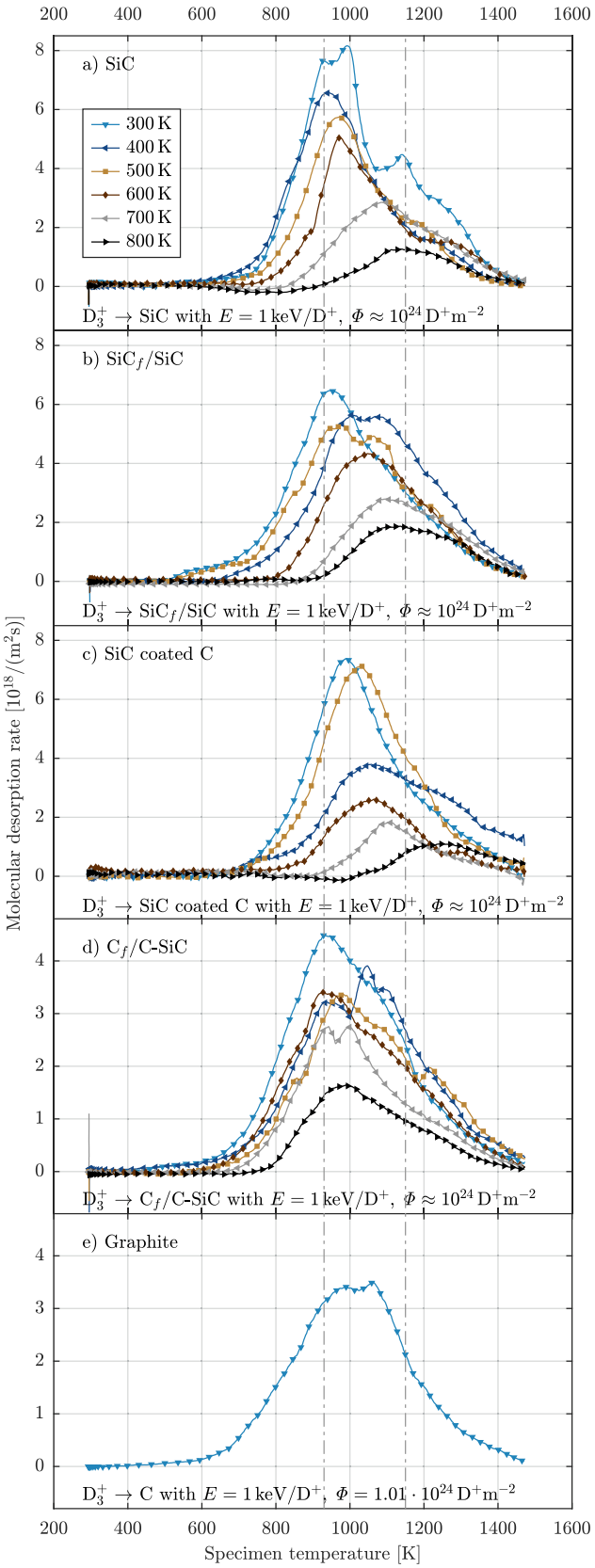

Fig. 3. TDS profiles of specimens irradiated at $E = 1$ keV/D$^+$ and $\Phi \approx 10^{24}$ D/m^2 and variable temperatures.

which can be absorbed in the porous surface layer of C_f/C-SiC. The two gray, vertical, dashed lines indicate the approximate location of the primary Si-D peak as mentioned before at about 930 K and the more vaguely visible secondary C-D peak at approximately 1150 K. While the primary peak lines up almost perfectly for SiC, SiC$_f$/SiC and C_f/C-SiC, the SiC coated graphite curve might be offset by about 50 K as it would be for a thermocouple with a slightly lower temperature reading. Moreover, curve a)-c) show signs of a shoulder on the right side of of the primary peak in the region where the C-D peak would be expected. Whilst obtained at the same experimental conditions, the SiC TDS curve depicted in Fig. 2 a) is different from the one shown in Fig. 1 in the sense that it does exhibit a shoulder instead of a distinct peak.

A composition of D_2 desorption curves as a function of implantation temperature for each investigated material is shown in Fig. 3. Curve a)–c) show both a decrease in the total amount of retained deuterium as well as a shift of the maximum towards higher temperatures with higher implantation temperature. This can be explained by the fact that Si-D bonds are increasingly unstable at elevated temperatures while C-D bonds can still be formed. This behaviour is confirmed by earlier measurements on SiC [5], SiC$_f$/SiC [6] and SiC coated graphite [7]. In contrast to the materials with a significant amount of SiC in the near surface area, the C_f/C-SiC curve of Fig. 3 d) shows only a decrease in the amount with no shift in the peak position. While the 300 K curve shows a rather SiC like shape with a peak at 950 K, other curves rather resemble graphite with a plateau like structure containing a small dip in the center such as the 400 K and 700 K C_f/C-SiC curves. This dip was previously seen in the graphite data of Mayer et al. [3] and might indicate that a certain variance resulting from samples with a different ratio between carbon fibres and SiC matrix within the area of the irradiation spot is present.

All individual TDS profiles are integrated over the full temperature range in order to obtain the total amount of retained deuterium. These results are plotted against the ion fluence, the particle energy or the substrate temperature in Fig. 4–6, respectively. Trend lines serve as a guide to the eye. In addition, error bars indicate a representative error estimation composed of the mean square error of the trend line to a 20% uncertainty leak bottle quantification error.

Fig. 4 shows the fluence dependent retention of sintered SiC in comparison with data on SiC from Oya et al. [4] as well as data on pyrolytic graphite from Haasz and Davis [13]. The data from Oya et al. was sampled at a higher particle energy of 2 keV/D$^+$ and was adjusted from D/SiC to D/m^2 values by multiplying the molecular density of SiC and twice the average range of deuterium ions in SiC of about 30.4 pm

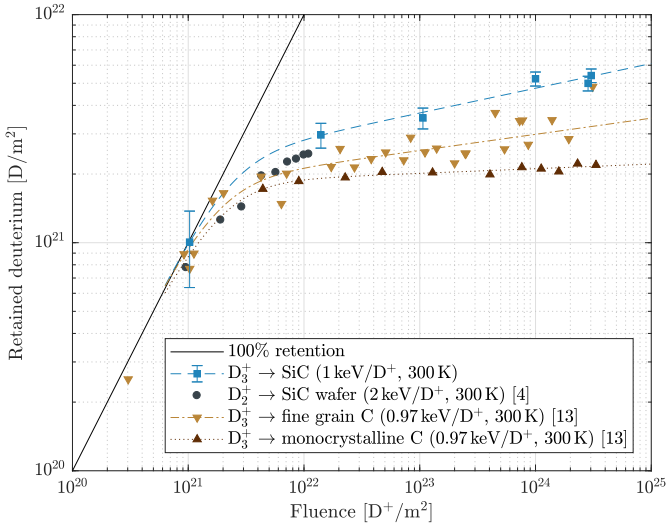

Fig. 4. Fluence dependence of the deuterium retention in SiC and pyr. graphite [4,13].

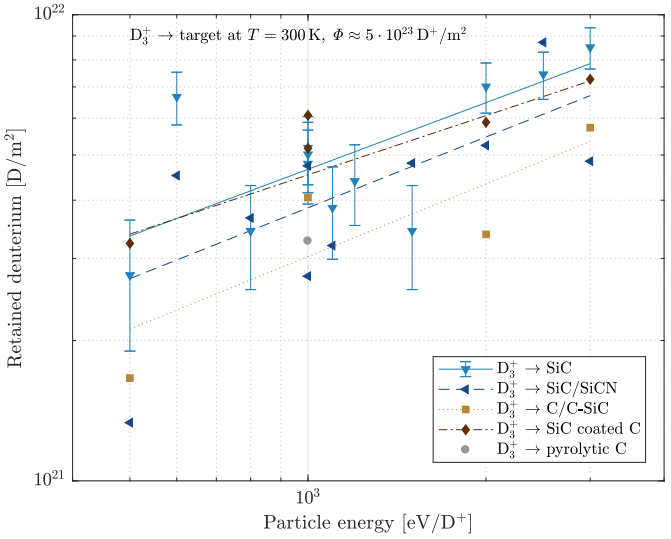

Fig. 5. Energy dependence of deuterium retention in SiC, SiC$_f$/SiC, C_f/C-SiC and SiC coated graphite.

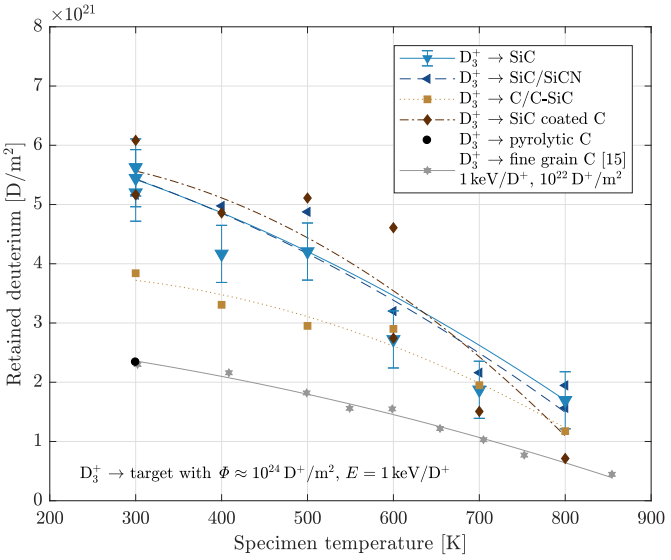

Fig. 6. Temperature dependence of deuterium retention in SiC, SiC$_f$/SiC, C_f/C-SiC, SiC coated graphite and pyrolytic graphite [15].

as estimated with the Stopping and Range of Ions in Matter (SRIM) code [14]. All curves show that the transition between 100% deuterium retention to a saturated state occurs within the same order of magnitude. As expected, the deuterium retention in bulk SiC is slightly higher than the literature results on graphite.

The energy dependence of the deuterium retention process is displayed in Figure 5. The gradient of the SiC, SiC$_f$/SiC and C/C-SiC log-log trend curves is close to 0.5 indicating that the total amount of retained deuterium is proportional to the square root of the particle energy during implantation. This is the expected behaviour since the main influence of the particle energy is to increase the range of the ions within the target material. While bulk SiC, SiC$_f$/SiC and SiC coated graphite are within the margin of error of each other, C_f/C-SiC exhibits a slightly lower deuterium retention behaviour.

Figure 6 shows the substrate temperature dependence of the deuterium retention in the tested materials as well as a comparison with pyrolytic graphite as obtained by Haasz and Davis [15]. Since their data was obtained at a fluence of $\Phi = 1.5 \cdot 10^{22}$ D/m^2 it is likely to be about 20% lower in magnitude. Overall, all curves show a decrease in

retention with increasing substrate temperature. Bulk SiC and SiC_f/SiC have an almost matching trend line while SiC coated graphite shows a sharper decrease at elevated temperatures. The amount of deuterium retained in C_f/C-SiC is, again, noticeably smaller than in SiC, yet higher than in pyrolytic graphite. An important observation is that the difference in deuterium retention at high substrate temperatures is small for all tested materials.

4. Conclusion

The total amount of retained deuterium is similar for all investigated materials with a significant silicon content at the surface (bulk SiC, SiC coated graphite and SiC_f/SiC) whereas C_f/C-SiC shows results in-between SiC and pyrolytic graphite. Neither the fibres nor the porosities seem to foster retention indicating that effects on the lattice scale such as vacancies and interstitials are more important to the trapping of deuterium than microscopic characteristics such as porosities. Further, the desorption of hydrocarbons seems to be irrelevant for SiC based ceramic materials in contrast to graphite and carbon composite materials. Increasing the particle energy and fluence increases the hydrogen retention whereas increases in the substrate temperature leads to less retention. The difference in the amount of retained deuterium between graphite and the tested SiC materials decreases at higher substrate temperature. Overall, the hydrogen retention in the various SiC materials is similar to retention in graphite within a factor of two over the entire range of parameters investigated. This means that the question if SiC is a suitable alternative to graphite should be decided by other parameters such as erosion, codeposition, plasma impurities or the mechanical properties.

Declaration of Competing Interest

The authors declare that they have no known competing financial interests or personal relationships that could have appeared to influence the work reported in this paper.

Acknowledgements

The help of the retired UTIAS technician C. Perez for handling and cutting the ceramic materials was greatly appreciated.

References

[1] L.H. Rovner, F.R. Hopkins, Ceramic materials for fusion, Nucl. Technol. 29 (3) (1976) 274–302, https://doi.org/10.13182/NT76-A31593.
[2] A.R. Raffray, L. El-Guebaly, S. Malang, I. Sviatoslavsky, M.S. Tillack, X. Wang, Advanced power core system for the ARIES-AT power plant, Fusion Eng. Des. 80 (1) (2006) 79–98, https://doi.org/10.1016/j.fusengdes.2005.06.356.
[3] M. Mayer, M. Balden, R. Behrisch, Deuterium retention in carbides and doped graphites, J. Nucl. Mater. 252 (1) (1998) 55–62, https://doi.org/10.1016/S0022-3115(97)00299-7.
[4] Y. Oya, K. Kawaai, K. Morita, K. Iinuma, K. Okuno, S. Tanaka, Y. Makide, Retention and re-emission behavior of hydrogen isotopes in SiC, Phys. Scr. T103 (2003) 81–84, https://doi.org/10.1238/Physica.Topical.103a00081.
[5] Y. Oya, Y. Onishi, K. Okuno, S. Tanaka, Trapping and detrapping mechanisms of deuterium in SiC studied by XPS and TDS techniques, J. Mat. Trans. 46 (3) (2005) 552–556, https://doi.org/10.2320/matertrans.46.552.
[6] Q. Li, W. Wang, Z. Yang, M. Kobayashi, M. Suzuki, J. Osuo, A. Hamada, K. Matsuoka, R. Kurata, J. Wu, C. Xie, L. Zhao, K. Okuno, Y. Oya, G. Luo, Deuterium retention in SiC coated graphite by D_2^+ implantation, Fusion Eng. Des. 86 (9) (2011) 1689–1692, https://doi.org/10.1016/j.fusengdes.2011.03.034.
[7] Y. Nobuta, T. Hino, Y. Yamauchi, T. Nozawa, Deuterium retention properties of SiC/SiC composites as plasma facing materials for fusion reactors after deuterium irradiation at elevated temperatures, J. Vac. Soc. Jpn. 58 (5) (2015) 173–176, https://doi.org/10.3131/jvsj2.58.173.
[8] R.A. Causey, J.D. Fowler, C. Ravanbakht, T.S. Elleman, K. Verghese, Hydrogen diffusion and solubility in silicon carbide, J. Am. Ceram. Soc. 61 (5-6) (1978) 221–225, https://doi.org/10.1111/j.1151-2916.1978.tb09284.x.
[9] G.A. Esteban, A. Perujo, F. Legarda, L.A. Sedano, B. Riccardi, Characterisation of deuterium transport in the fibres and matrix of a 3D-SiC_f/SiC composite, Fusion Eng. Des. 69 (1-4) (2003) 463–467, https://doi.org/10.1016/S0920-3796(03)00103-0.
[10] B. Mainzer, C. Lin, R. Jemmali, M. Frieß, R. Riedel, D. Koch, Characterization and application of a novel low viscosity polysilazane for the manufacture of C- and SiC-fiber reinforced SiCN ceramic matrix composites by PIP process, J. Eur. Ceram. Soc. 39 (2) (2018) 212–221, https://doi.org/10.1016/j.jeurceramsoc.2018.09.042.
[11] M. Frieß, W. Krenkel, R. Brandt, G. Neuer, Influence of process parameters on the thermophysical properties of C/C-SiC, High Temp. Ceram. Matrix Compos. (2001) 328–333, https://doi.org/10.1002/3527605622.ch52.
[12] A.A. Haasz, J.W. Davis, Synergistic chemical erosion of graphite due to simultaneous bombardment by H+ and other low-Z ions using a dual-beam accelerator, Nucl. Instrum. Methods Phys. Res. Sect. B 83 (1993) 117–124, https://doi.org/10.1016/0168-583X(93)95915-R.
[13] A.A. Haasz, J.W. Davis, Fluence dependence of deuterium trapping in graphite, J. Nucl. Mater. 209 (2) (1994) 155–160, https://doi.org/10.1016/0022-3115(94)90290-9.
[14] J.F. Ziegler, M.D. Ziegler, J.P. Biersack, SRIM the stopping and range of ions in matter (2010), Nucl. Instrum. Methods Phys. Res. Sect. B 268 (11) (2010) 1818–1823, https://doi.org/10.1016/j.nimb.2010.02.091.
[15] A.A. Haasz, J.W. Davis, Deuterium retention in doped graphites, J. Nucl. Mater. 232 (2) (1996) 219–225, https://doi.org/10.1016/S0022-3115(96)00395-9.